Proceedings of the 10th International Conference on Fluid Flow, Heat and Mass Transfer (FFHMT'23)
Ottawa, Canada – June 07-09, 2023
Paper No. 172
DOI: 10.11159/ffhmt23.172

Numerical Study of Transverse Pitch Effect On Pressure Loss In An Inline Array Of Elliptical Pins

Justina Jaseliūnaitė[1], Marijus Šeporaitis[1],
[1]Lithuanian Energy Institute, Laboratory of Nuclear Installation Safety
Breslaujos st. 3, Kaunas, Lithuania
justina.jaseliunaite@lei.lt; marijus.seporaitis@lei.lt

Abstract **-** The internal geometrical parameters of the pin-fin arrays have a significant influence on its performance. This paper presents a three-dimensional numerical analysis of pin-fin arrays where only a small part of the channel is modelled by applying cyclic boundary conditions. The simulations are performed using the computational fluid dynamics software OpenFOAM v10. The results are validated against real experimental data and previous two-dimensional study. Furthermore, in order to address the lack of consistent research data on the influence of the pin spacing, this study aims to systematically model and investigate the hydraulic performance of pin-fin array by changing the transverse pitch slightly while keeping the longitudinal pitch, the diameter of the pins, and the height of the channel unchanged. For an inline layout of elliptical pin-fins, it was found that the optimum ratio between the transverse spacing and the width of the pins should be between 1 and 1.5.

Keywords**:** pin-fin array, CFD, pressure drop, flow characteristics, transverse pitch

1. Introduction

Overheating is the main cause of damage to modern smart devices, followed by vibration, moisture and dust [1]. Electronic components generate a lot of heat during operation. Too much heat energy can damage devices, so their performance and longevity depend heavily on their ability to dissipate heat. Compact heat exchangers (CHE) with a high heat transfer surface-to-volume ratio have been introduced to address this problem. CHEs are available in a variety of geometric configurations, such as a flat plate or a pin fin. Regardless of the type of pin fins, they still enhance heat transfer [1, 2, 3].

Perhaps the most common CHE design is the pin-fin array, where fin shape types include, but are not limited to, cylinder, square, triangle, ellipse, cone, and drop. The most efficient fin shape is considered streamlined since it creates the lowest pressure drop and keeps the flow stable longer [4, 5, 6]. Furthermore, the layout has a significant impact on the performance of CHE only when the Re number is high. On the other hand, at a low Re, differences between layouts have a negligible effect on performance because the emerging disturbances are suppressed in the staggered array [7]. Therefore, heat transfer is not enhanced by unsteady vortices [2]. Flow through inline layout is characterized by high-velocity mainstream between the pins as well as the double vortices behind the pins [7]. Therefore, efforts are being made to make the stagnant vortices as small as possible and keep the flow stable.

Generally, the more densely spaced the pins, the greater the heat transfer capacity [8]. Cormier et al. [9] conducted a numerical study on the effect of pin-fin spacing on thermohydraulic performance. The results showed that densely arranged pin-fins lead to higher pressure drop as well as better thermal performance. In addition, the effect of altering transverse and longitudinal spacing is different. The increase in longitudinal pitch increases resistance to the air flow and thermal efficiency. At higher flow rates, a larger longitudinal pitch gives considerably higher efficiency [10] as the flow is unstable and the mixing in an area between pins is higher [8]. On the other hand, at lower Re, a lower longitudinal pitch is considered to have better thermohydraulic performance. While the increase of transverse pitch decreases the heat transfer coefficient and the pressure loss, the reason for this was indicated as swirling flow promotion and delayed wake instabilities due to the smaller transverse pitch [8, 11].

If pins do not extend the full height of the channel, the gaps increase vorticity, which results in reduced convective heat transfer. Even at the base, where there is no gap, heat removal is worse, while pressure losses in the channel are much higher, making this design less appealing [12]. Ates et al. [13] concluded that a heatsink without gaps above the pins is more efficient.

Regarding pin diameter, although the spacing between pins is the same, a smaller diameter leads to faster flow instability as well as lower pressure losses. However, the influence of the pressure drop due to the hydraulic boundary layer effect caused by the end walls is greater in a sparse pin array [14].

From the above discussion, it can be seen that most of the research has been carried out on different pin-fin layouts and geometries. No conclusion has been drawn as to which is the best configuration, just some guidelines. The objective of this study is to find out more about the optimisation of pin arrays in the light of previous studies. This time, the study is conducted by 3D simulations, considering the influence of the end walls, and is compared with the results of the 2D study [4]. Also, the influence of the transverse pitch of the elliptical pins on the pressure drop is analysed more extensively.

2. Methodology

The simulations were conducted for a cylindrical pin-fin array, the dimensions of which were the same as those of the inline pin-fin array studied by Renfer et al. [15]. A schematic diagram of the pin-fin array is shown in Fig 1. The channel height, length, and width are 200 μm, 0.01 m, and 0.01 m, respectively. The transverse and longitudinal pin pitch are 200 μm, and the pin diameter is equal to 100 μm. The pin fin array consists of 50 pins in both longitudinal and transverse directions. The fluid used is room-temperature water.

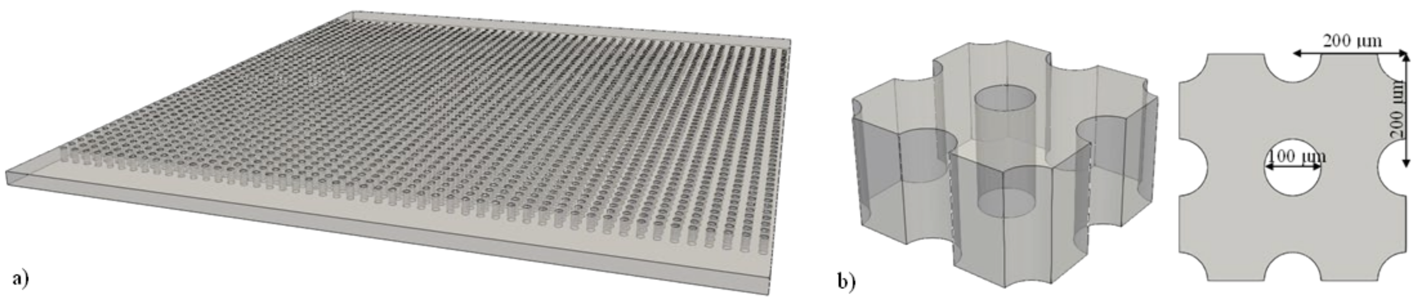

Fig. 1: The geometry of cylinder micro pin-fin array a) entire channel, b) part of the channel.

2.1. Numerical model

In this study, three-dimensional Reynolds averaged Navier Stokes equations are solved. The flow is assumed incompressible, three-dimensional, adiabatic, and Newtonian.

The open-source CFD software OpenFOAM v10 is used for the numerical study, PISO algorithm is used to couple pressure and velocity fields. The second-order linear scheme was used for spatial discretization. Gradients are computed using a linear scheme. K-ω SST turbulence model is selected for turbulence simulation.

2.2. Computational domain and mesh

Since the pin-fin geometry are periodic in both the transverse and longitudinal directions, cyclic boundary conditions have been selected. It is assumed that the flow is fully developed, thus, the flow exiting the domain is fed back to the inlet. This section can be considered an infinitely long cascade of such elements connected together.

The pin-fins, as well as the upper and lower walls, have a no-slip boundary condition. The computational domain is shown in Fig 1 a), which is consistent with the experimental geometric specifications [15]. The whole computational domain consists of structured hexahedron mesh elements. The numerical simulations were run at Reynolds number starting from 50 to 250. The reference length of Reynolds number is defined by the diameter of the pins.

Ten different configurations of elliptical pin-fins are used in this research which are introduced with abbreviations in Table 1. The D(x/y) letter regards conjugate diameter in x and y directions, namely Px for longitudinal spacing and Py for transverse spacing. Two of the elliptical pin-fin arrays have been investigated in the previous article [4] but in the 2D case. Therefore, they were selected as the most conspicuous cases, and the new ones have transverse pitches starting from 50 μm to 140 μm.

Table 1: Specification of cases.

Name	Conjugate pin diameter (x-axis), *Dx*, µm	Conjugate pin diameter (y-axis), *Dy*, µm	Longitudinal spacing, *Px*, µm	Transverse spacing, *Py*, µm
D100-Px200-Py200	100	100	200	200
Dx100-Dy40-Px200-Py50	100	40	200	50
Dx100-Dy40-Px200-Py60	100	40	200	60
Dx100-Dy40-Px200-Py70	100	40	200	70
Dx100-Dy40-Px200-Py80	100	40	200	80
Dx100-Dy40-Px200-Py90	100	40	200	90
Dx100-Dy40-Px200-Py100	100	40	200	100
Dx100-Dy40-Px200-Py110	100	40	200	110
Dx100-Dy40-Px200-Py120	100	40	200	120
Dx100-Dy40-Px200-Py130	100	40	200	130
Dx100-Dy40-Px200-Py140	100	40	200	140

2.3. Validation of the computational model

The grid independence of the simulation results has been tested on an array of cylindrical pin-fins using six meshes of different fineness, with element sizes ranging from 11 to 3.5 µm. Fig. 2 shows how the simulated pressure drop depends on the number of mesh elements. It was found that the effect of further mesh refinement on the result becomes negligible when the mesh contains 435 200 elements with a size of 4 µm. Therefore, the number of elements in the other meshes for further simulations was chosen to be 435 200. For all array configurations investigated in this work, the size of the elements was the same or lower.

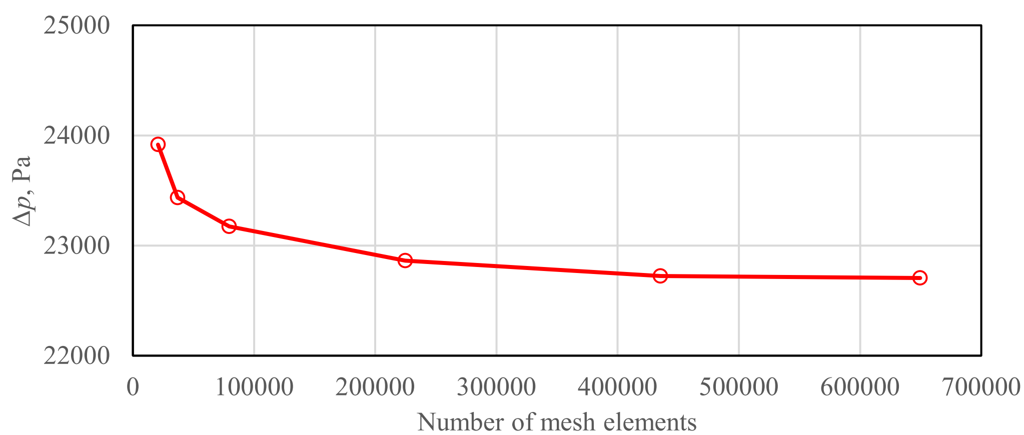

Fig. 2: Grid independence test.

The simulation results are compared with experimental data from Renfer et al. [15] (See Fig. 3). Naturally, the endwalls affect the flow by forming a boundary layer. Ji et al. [7] reported that, due to the flow-restricting upper and lower walls, vortex shedding starts further downstream, which, as expected, shows up in progressing from 2D to 3D simulations. Thus, the differences between the compared cases are logical and acceptable, and the study is valid.

The statistical metric that defines the accuracy of a prediction method, the Mean Absolute Percentage Error (MAPE), is used to determine the percentage error between numerical results and experimental data. The average discrepancy of pressure drop is 13 % but given that cyclic boundary conditions are used in the model. It is concluded that the results are in good agreement with the experimental data.

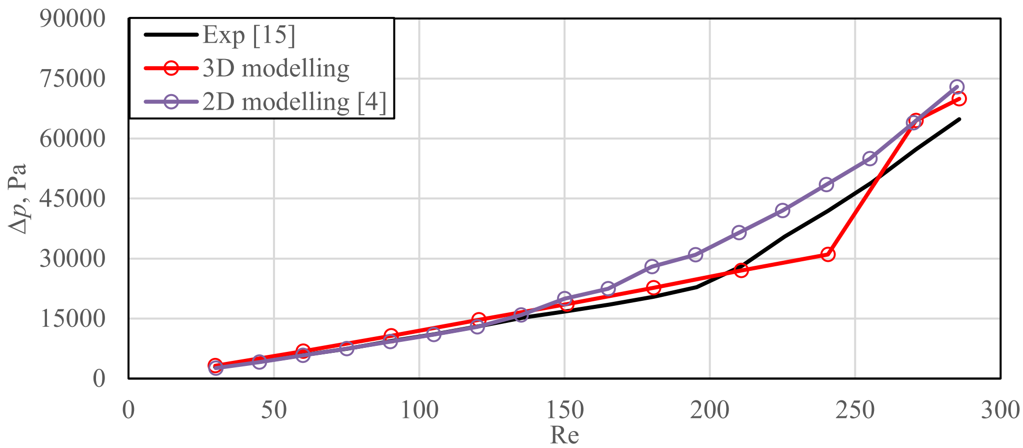

Fig. 3: Comparison between numerical results and experimental data.

3. Results

The main objective of this work was to investigate the effect of the transverse pitch of the pin fins with elliptical cross-sections. Typical laminar flow patterns can be seen in Fig 4. The larger the transverse pitch *Py*, the smaller the pair of stagnant vortices behind the pins. And the smaller the *Py*, the more accelerated the flow between adjacent pins.

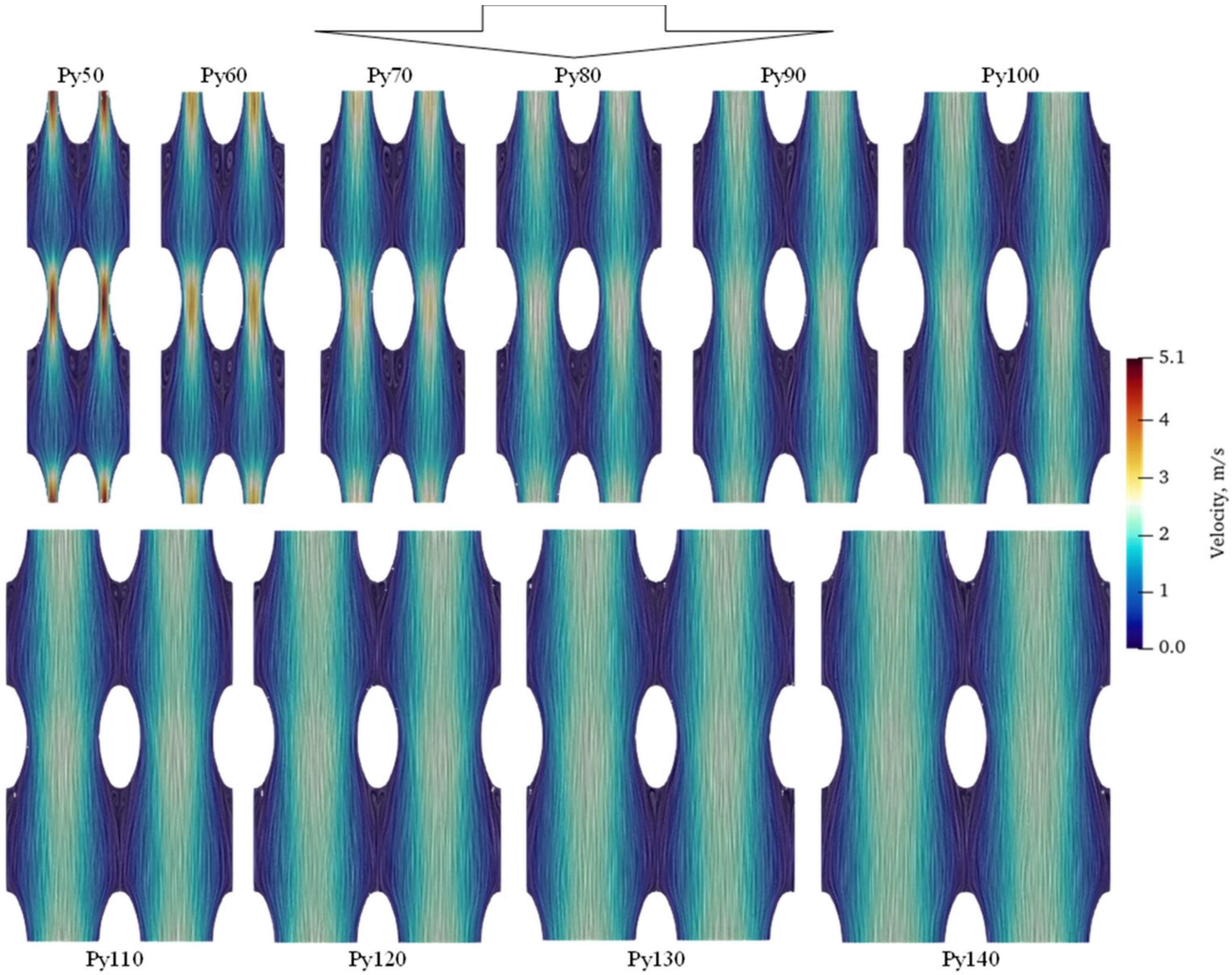

Fig. 4: Flow field of Dx100-Dy40-Px200-Py50 – Py140

The influence of *Py* on the non-dimensional pressure drop (p^*) is shown in Fig. 5. The pressure drop was non-dimensionalized by using the pressure drop value in a configuration with the same pin pitch in both directions (*Px* = *Py* = 200 µm). Obviously, the pressure drop increases with decreasing *Py* as the blockage ratio (*BR*) increases. However, the pressure drop increase trend is different from the parabolic increase in *BR* with decreasing *Py*. This can be explained by flow separation: - as the flow velocity between the pins increases, the boundary layer becomes thinner, and its separation points move upstream. The exponential response of the pressure drop to *BR* can be described by:

$$p^* = 0.032023 \cdot e^{9.9906 \cdot BR} + 1.7833 \quad (1)$$

Increasing the transverse pitch to and beyond *Dx* results in almost no reduction in pressure drop. This is because the boundary layer separation point and the vortices behind the pins remain almost unchanged while the velocity between adjacent pins continues to decrease. Therefore, a comparison of the rates of change of the relative pressure drop p* and the relative surface area (SA), as in Figure 6, is suitable for assessing the expected thermo-hydraulic performance of the array. It can be seen that the most efficient of the configurations investigated is the one with *Py* = *Dx* (100 µm). Still, a ratio of *Py* = 0.8*Dx* can be quite reasonably used to achieve higher thermal performance.

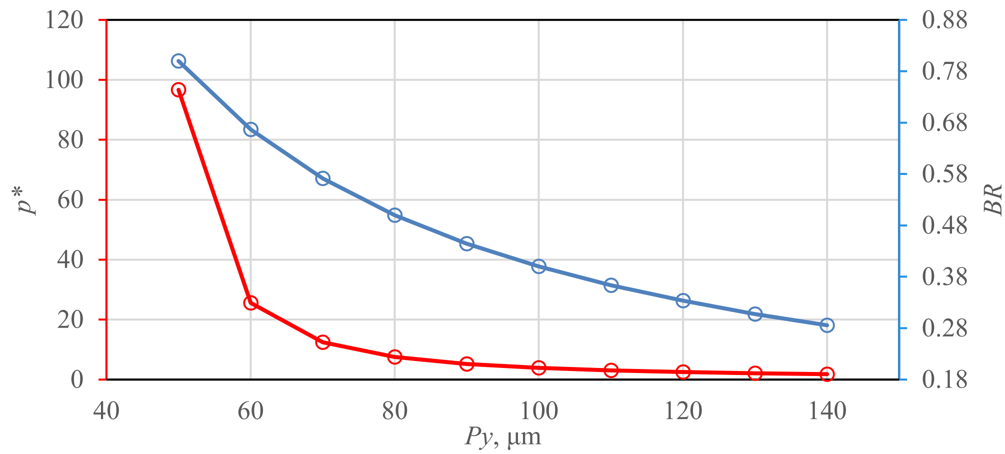

Fig. 5: Non-dimensional pressure drop versus blockage ratio dependence on transverse pitch (u_{mean} = 1 m/s, Re = 353.7).

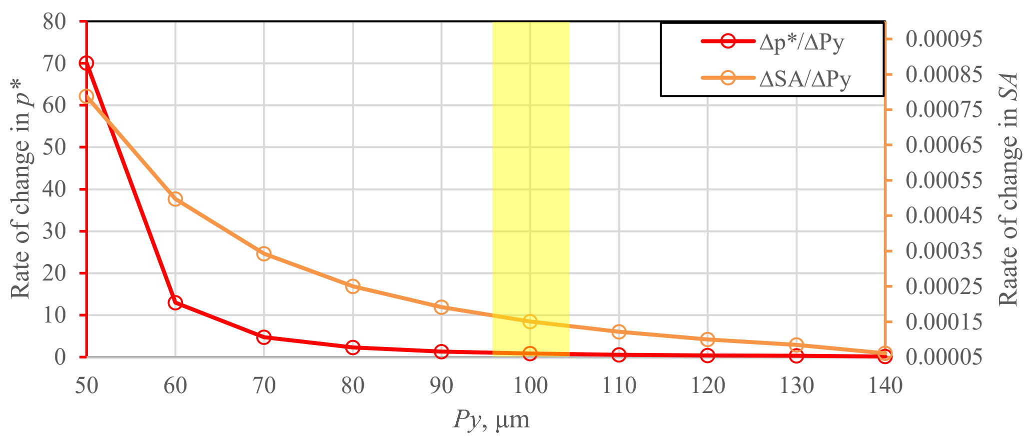

Fig. 6: Rate of change in p^* vs. *SA* (ΔPy = 10 µm). The yellow area marks the most effective pitch.

4. Conclusion

In this study, numerical simulations were performed to obtain pressure drop results for different pin-fin array configurations, with a particular focus on elliptical pins having different transverse pitches. The numerical model has been validated against experimental results and is consistent with previous research. Three-dimensional numerical simulations with different transverse pitches of the pins showed an exponential increase in pressure drop with increasing *Py*. An exponential formula was analytically derived, which estimates the dependence of the non-dimensional pressure drop on the blockage ratio. Of all the elliptical pins with different *Py* configurations investigated, the Py100 case was found to be the best due to its low pressure loss with a still large surface area.

Nomenclature

BR – blockcage ratio
Dx – pin diameter in x axis
Dy – pin diameter in y axis
Py – transverse spacing
Px – longitudinal spacing
Δp – pressure drop

p^* – non-dimensional pressure drop
Re – Reynolds number
SA – relative surface area

References

[1] A. Moradikazerouni, "Heat transfer characteristics of thermal energy storage system using single and multi-phase cooled heat sinks: A review," *J Energy Storage.,* vol 49, pp. 104097, 2022.

[2] Y. Qiu, W. Hu, C. Wu and W. Chen, " An Experimental Study of Microchannel and Micro-Pin-Fin Based On-Chip Cooling Systems with Silicon-to-Silicon Direct Bonding," *Sensors*, vol. 20, pp 5533, 2020.

[3] M. Z. Saghir and M. M. Rahman, "Thermo-Hydraulic Performance of Pin-Fins in Wavy and Straight Configurations,", *Micromachines,* vol. 13, pp. 954, 2022.

[4] J. Jaseliūnaitė and M. Šeporaitis, "Performance Optimization of Microchannel Pin-Fins using 2D CFD", *Appl Therm Eng*, vol. 206, pp. 118040, 2022.

[5] N. K. Al-Abboodi, K. A. Khalaf, H. Ridha and M. G. Al-Azawy, "Thermal and Flow Analysis of Different Shaped Pin Fins for Improved Heat Transfer Rate," *Int J Heat Technol*, vol. 40, no. 1, pp. 201-210, 2022.

[6] F. Wang, J. Zhang and S. Wang, " Investigation on flow and heat transfer characteristics in rectangular channel with drop-shaped pin fins," Propuls Power Res, vol. 1, no. 1, pp. 64-70, 2012.

[7] C. Ji, Z. Liu and M. Lv, "Micro-particle image velocimetry study on hydrodynamic characteristics of inline and staggered micro pin fin arrays", *Chem Eng Process,* vol. 179, pp. 109058, 2022.

[8] A. Rozati, D. K. Tafti and N. E. Blackwell, "Thermal Performance of Pin Fins at Low Reynolds Numbers in Mini-Micro-Channels," *Proceedings of 2007 ASME-JSME Thermal Engineering Summer Heat Transfer Conference,* Vancouver, Canada, 2007.

[9] Y. Cormier, P. Dupuis, A. Farjam, A. Corbeil and B. Jodoin, "Additive manufacturing of pyramidal pin fins: Height and fin density effects under forced convection," *Int J Heat Mass Transf,* vol. 75, pp. 235-244, 2014.

[10] M.S. Manjunath, K. V. Karanth and N. Y. Sharma, "Numerical Analysis of Flat Plate Solar Air Heater Integrated with an Array of Pin Fins on Absorber Plate for Enhancement in Thermal Performance.," *J Sol Energy Eng*, vol. 141, pp. 5, 2019.

[11] N. B. Sukhor, A. S. Tijani, J. Kubenthiran and I. K. Muritala, "Computational modeling of thermal characteristics of hybrid nanofluid in micro-pin fin heat sink for electronic cooling," *Int J Green Energy,* vol. 18, no. 10, pp. 1027-1045, 2021.

[12] A. Shahsavar, M. Shahmohammadi and I. B. Askari, "CFD simulation of the impact of tip clearance on the hydrothermal performance and entropy generation of a water-cooled pin-fin heat sink," *Int Commun Heat Mass Transf,* vol. 126, pp. 105400, 2021.

[13] A. Ates, B. P. Benam, V. Yagci, M. C. Malyemez, M. Parlak, A. K. Sadaghiani and A. Kosar, "On the effect of elliptical pin Fins, distribution pin Fins, and tip clearance on the performance of heat sinks in flow boiling," *Appl Therm Eng,* vol. 212, pp. 118648, 2022.

[14] D. Guo, J. Gao, S. Santhanam and S.C. Yao, "Experimental investigation of laminar flow across short micro pin fin arrays," *J Micromech Microeng*, vol. 24, pp. 095011, 2014.

[15] A. Renfer, M. K. Tiwari, T. Brunschwiler, B. Michel and D. Poulikakos, "Experimental investigation into vortex structure and pressure drop across microcavities in 3D integrated electronics," *Exp Fluids,* vol. 51, no. 3, pp. 731-741, 2011.